International Journal of Concrete Structures and Materials

RESEARCH

Open Access

Experimental Investigation on Axial Strength Improvement of Cold-Formed Steel Jacketed Concrete Stub Columns

Apisith Waenpracha[1], Tanyada Pannachet[1,2*] and Maetee Boonpichetvong[1,2]

Abstract

This paper presents an experimental study on the behavior of low-strength concrete columns confined with cold-formed steel under axial compression. The laboratory test specimens consist of four groups of rectangular concrete stub columns in the size of 130 × 200 mm cross section and 300 mm height; the first group composes of the unconfined specimens, while the other three contain the confined specimens under 0%, 25% and 50% sustained axial loads. The jackets are made of two G450-grade channel cold-formed steel sections of 2.4 mm thickness welded together. No bonding material is used between the core concrete and the steel jacket. From the results, it is found that the cold-formed steel jacketing can increase the axial strengths of the unconfined concrete specimens by approximately 40-65%. The strength increase comes mainly from the confinement action, as only small axial deformation is detected in the jacket. Based on the given amount of prescribed preloads in this study, the presence of preload in the column does not have a significant effect on the increase in strength of the confined concrete columns. The measured strength enhancement ratio and the confinement ratio of the tested specimens are compared using five existing strength predictive equations. The performance of the unbonded cold-formed steel jacketing technique adopted in the stub columns is observed to closely conform with the predictive confinement model of the concrete-filled tubes.

Keywords Cold-formed steel, Confinement, Preload, Low-strength concrete, Axial compression

1 Introduction

Reinforced concrete buildings that have been in service for a long time frequently experience a variety of issues. Either it is due to material degradation, change of building functions, or emergence of new design standards, there are needs that building structures or various structural components must be strengthened in order for them to resist forces safely. Strengthening techniques may be either modifying the overall structure by including new elements to improve force distribution in the structure, or merely modifying some structural components that are likely to reach or exceed their force resistance capability (Thermou et al., 2012). While the global strengthening techniques can successfully upgrade performance of structures, the local strengthening techniques have some advantages for their simpler installation.

One of the popular techniques that is commonly used in upgrading axial compression capability of a concrete column is to provide lateral confinement to the column; the confining material acts as a jacket to the core concrete. In general, the confining material must have a high tensile strength along the circumferential direction so that it can help resisting lateral expansion that occurs in

Journal information: ISSN 1976-0485 / eISSN 2234-1315

*Correspondence:
Tanyada Pannachet
tanpan@kku.ac.th
[1] Department of Civil Engineering, Faculty of Engineering, Khon Kaen University, Khon Kaen 40002, Thailand
[2] Sustainable Infrastructure Research and Development Center, Khon Kaen University, Khon Kaen 40002, Thailand

the column during axial compressive loading. At present, there are various types of materials used for jacketing concrete columns, including reinforced concrete (Ersoy et al., 1993; Minafó 2015), fiber-reinforced concrete (Elsayed et al., 2023), steel (Choi, 2009; Belal et al., 2015; Villar-Salinas et al., 2021), fiber-reinforced polymer (FRP) sheet (Mirmiran et al., 1998; Shahawy et al., 2000; Shehata et al., 2002; Almusallam, 2007), engineered cementitious composite (ECC) (Lai et al., 2023a, b, 2024), etc. Jackets made of concrete have an advantage over other confining materials in terms of fire resistance. Adding steel fiber to the concrete jacket also significantly improved the post-heated column capacity (Abo-Zaid et al., 2019). However, the thickness of the concrete jacket, even at its minimum requirement, may increase the size and weight of the building to the extent that it may cause a major change in force distribution in the building structure, and consequently affects details of the foundation and the architectural dimension of the building. This is why use of lightweight materials, such as the carbon fiber-reinforced polymer (CFRP) sheet, has become a preferred alternative in recent years. Despite its high cost, the CFRP sheet has a high tensile strength-to-weight ratio and also some corrosion resistance, which are suitable for many structural applications (Vijayan et al., 2023). However, CFRP itself often raises the durability issue and requires periodic maintenance.

Steel is another interesting alternative that has been commonly used for external confinement of concrete columns for decades. Steel jackets do not increase the column size or add the extra weight to the column as much as concrete jackets. Compared to the externally bonded CFRP system, the steel jacketing is of the lower cost and has the ductile material behavior that is sufficient to give warning sign before it fails. According to the reviews by Chin et al. (2019), there are mainly four types of steel confinement to concrete, including concrete-filled tubes and the other three types that provide external confinement to concrete, i.e., by a continuous piece of steel, by steel caging, and by steel straps. Under axial compressive loading, concrete-filled steel tube provides axial contribution with the concrete and confining action to the concrete, while the other three types are based only on the confining action.

Similar to the hot-rolled steel, the cold-formed steel can also be used to strengthen concrete in a variety of ways, including external bracing (Yu et al., 2024) and jacketing. The previous research works have mainly focused on application of cold-formed steel in the form of concrete-filled tube, in which the tube mainly contributes to the axial compression and somewhat to the confinement (Chen et al., 2023). The resulting improved axial capacity depended on the thickness of the cold-formed steel and the shape of the concrete section (Lin, 1988). For square and rectangle cross sections, the tensile properties of the cold-formed steel were found to be different on the flat portions and the corner portions (Men et al., 2024). It was also found that the confined concrete strength increased with the yield strength of the cold-formed steel but the confinement effectiveness decreased with the increase of the unconfined concrete strength (Wang et al., 2021). As the local buckling of the tubes also significantly reduced the confining effect, it was suggested to add welded stiffeners on the jacket (Huang et al., 2023), to create longitudinal stiffeners by arranging built-up patterns (Harrat et al., 2024; Zhang et al., 2024), or to place bonding material between the steel plate and the concrete (Taufiq and Lawson, 2020). Although being limited, there was also a work on using cold-formed steel sections for post-installation on concrete columns. In Kumar and Ramasamy (2017), two 1.4-mm-thick cold-formed steel hat sections were bolted together to confine the concrete columns of a predefined size, without applying any bonding material. The axial strengths of the columns were enhanced from 39-57% before failure by local crushing or vertical splitting at the middle section. Behavior of the concrete specimens confined with the very thin version of the cold-formed steel, which is known as the metal sheet, has also been investigated experimentally (Khamthong, 2012; Positong et al., 2018; Pannachet and Boonpichetvong, 2018) and numerically (Boonpichetvong et al., 2016, 2018; Pannachet and Boonpichetvong, 2019). In these works, the metal sheet as thin as 0.23 mm was wrapped around the concrete specimens. Using the epoxy resin as the bonding material, the improved stress–strain behavior of the specimens was not influenced by lateral confinement only, but also by ability of metal sheet in resisting axial compression along with the core. By using small strips instead of one large piece of metal sheet, local failure or wrinkles of the metal sheet could be avoided (Positong et al., 2018).

In this paper, external strengthening of concrete columns using cold-formed steel is further investigated. The work is based on the previous works of the authors that use the thinner cold-formed steel sections in the form of metal sheet to wrap around concrete columns. The motivation of this work comes from the observation that it requires more than one layer of thin metal sheet in order to get the column to the desired compressive strength. As it appears that the behavior of the confined concrete also depends on the thickness of the confining material, using a thicker version of cold-formed steel instead of many layers of thinner sheets tends to provide a benefit of simpler installation. Thus, the available research works have mainly put focus on the use of concrete-filled cold-form steel tube rather than the external jacketing

system. The cold-formed steel has some advantages to be another good alternative in the jacketing system; the sections are typically thin, therefore their lightweight facilitates the installation and do not add much weight to the existing structure. Other than that, the cold-formed steel products are always coated with aluminum–zinc, therefore higher durability than the hot-rolled steel can be expected.

The experiments given in the paper additionally take into account effect of axial preloads on compressive behavior of concrete columns, to address a crucial topic in strengthening practice. The vast majority of research in this subject is conducted without accounting for influence of the initial axial stress that practically exists in columns during jacket installation. The results from many research (Takeuti et al., 2008; Shi and He, 2009; Papanikolaou et al., 2013) have agreed that the sustained axial load in concrete columns before being jacketed could result in less improved compressive strength of the jacketed columns, due to the decreased confinement effect. However, it was found that extent of the strength reduction could be marginal under low preload stress level, but becomes more pronounced for higher preload levels (Shi and He, 2009; Papanikolaou et al., 2013; Micelli et al., 2021). The results in a series of research works (Ferrotto et al., 2018a, b, c, 2021), based on laboratory tests and numerical experiments, also revealed that the level of sustained loads at the time of jacketing could affect axial strength of the strengthened column, and consequently the total performance of the retrofitted structure. The effects became more significant for greater preloaded forces, as larger creep strains were developed resulting in micro-cracks in concrete and the strain-lag effects emerged in the confining material (Pan et al., 2017; Ferrotto et al., 2021). Some strength prediction equations that considered preload effects were proposed in (Pan et al., 2017; Micelli et al., 2021; Lu et al., 2022). In order to account for the service axial loads, our experimental test consisted of the test specimens that were not-preloaded as well as the specimens that were preloaded at two different levels before jacket installation. The results were also compared with the existing prediction equations.

2 The Test Specimens

In order to accomplish the objectives of our study, four groups of the test specimens, with three specimens in each group, were created. The first group consisted of the unconfined plain concrete specimens, to be used as the reference. The other three groups consisted of the plain concrete specimens that were put under three different levels of preload, including 0%, 25% and 50% preload levels, before being confined with cold-formed steel jackets. A preload level is defined as a percentage of the prescribed axial stress before installation of jacket on the specimen, in comparison to the axial compressive strength of the unconfined specimen. Details of the test specimens are summarized in Table 1.

As the primary goal was to examine the pure confinement effect utilizing cold-formed steel with a greater thickness than that of our prior studies, the jacketing system was created without any use of bonding materials so that there was no resistance in the axial direction in addition to the confinement. To be able to install the jacket as closely to the core concrete, the concrete was cast in the prebuilt jackets which were used later on for confining the concrete specimens of the predefined shape. Properties of the concrete and the cold-formed steel section, as well as the preparation of the concrete specimens in all the groups are described in the following subsections.

2.1 Concrete

The unconfined compressive strength of the standard cylindrical specimens was chosen to be around 17 MPa, representing concrete with a lower compressive strength after some period of usage. The designed concrete mix contained a water–cement ratio (w/c) of 0.56 and a slump of 100 mm, with the concrete mix ratio of 1.8:1:5:3.8 representing the proportion of Portland cement type 1:water:aggregates:sand, measured by weight. To obtain the mechanical properties of concrete, three standard cylindrical concrete samples, with the diameter of 150 mm and the height of 300 mm, were tested in accordance with ASTM C39 (2021) and ASTM C469 (2022) at 28 days. As a result, the averaged compressive strength obtained from six standard cylindrical concrete samples was 17.85 MPa.

2.2 Cold-Formed Steel Section

The cold-formed steel section used in this study was selected from the sections that are available in the market in Thailand. As one of the most widely used cold-formed steel products, a lipped channel cold-formed steel section was selected. The section, specified as C20024 with

Table 1 The test specimens

Group	Confining material	Level of preloading	Specimens in the group
C0	None	None	C0-1, C0-2, C0-3
CJ0	Cold-formed steel	0%	CJ0-1, CJ0-2, CJ0-3
CJ25	Cold-formed steel	25%	CJ25-1, CJ25-2, CJ25-3
CJ50	Cold-formed steel	50%	CJ50-1, CJ50-2, CJ50-3

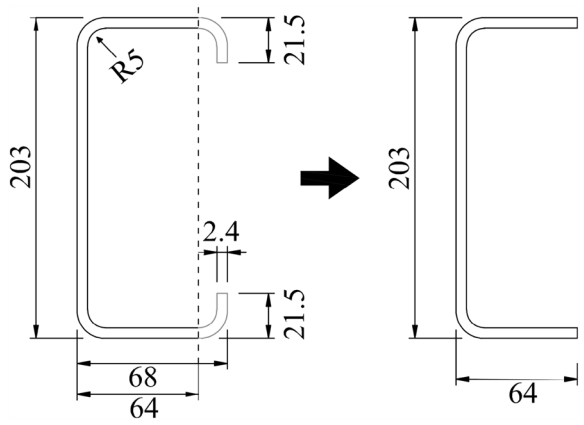

Fig. 1 Geometrical properties of the original C20024 cold-formed steel section (left) and the cut section (right). [Unit in mm.]

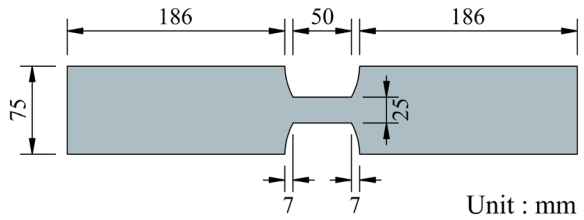

Fig. 2 Size of the cold-formed steel samples for tensile testing

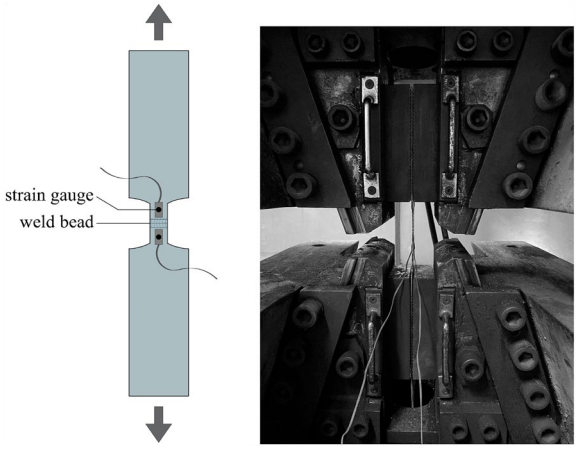

Fig. 3 The tensile testing

Table 2 The tensile strengths of the cold-formed steel samples

Group	Sample	Yield strength (MPa)	Ultimate strength (MPa)
Continuous (one-piece) Samples	SC-1	572.4	602.3
	SC-2	595.5	624.8
Welded (two-piece) Samples	SW-1	446.3	482.6
	SW-2	289.4	311.4

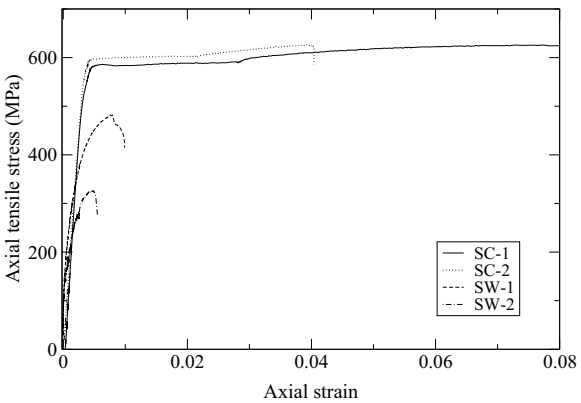

Fig. 4 The tensile stress–strain relationships of the cold-formed steel samples

the steel grade G450, has the minimum yield strength of 450 MPa according to the standard tests AS/NZS 1365 (2016), AS 1397 (2021) and JIS 3323 (2022). The geometrical properties of the section are specified in Fig. 1(left).

To examine the tensile properties of the cold-formed steel materials used in this study, the test samples were prepared following the requirements of the standard test methods for tension testing of metallic materials (ASTM E8/E8M) (2022) to determine the tensile strengths at yield and peak, as well as the modulus of elasticity. In total, four test samples were divided into two groups, consisting of continuous (one-piece) samples and welded (two-piece) samples, of which the size and shape are as shown in Fig. 2. The tension testing was conducted using a universal testing machine. As shown in Fig. 3, one 5-mm strain gauge was placed at the middle of the length for the one-piece samples, whereas two strain gauges were installed next to each side of the weld line for the welded samples. All the strain gauges were aligned along the loading direction.

The tensile strengths of the four samples are collected in Table 2, and the tensile stress–strain relationships of the specimens are shown in Fig. 4. The failure was observed at a position on the narrow part of all the specimens, and exactly on the weld line in case of the welded test specimens, as shown in Fig. 5. The results from the tensile testing of the continuous pieces revealed the ductile material behavior, with the yield strengths around 580 MPa and the ultimate strengths around 610 MPa. The results from the welded specimens, on the other hand, reported the non-consistent values of the strengths, and also the brittle failures at the weld line. The weld strengths ranged from 50% to 75% of the steel strengths.

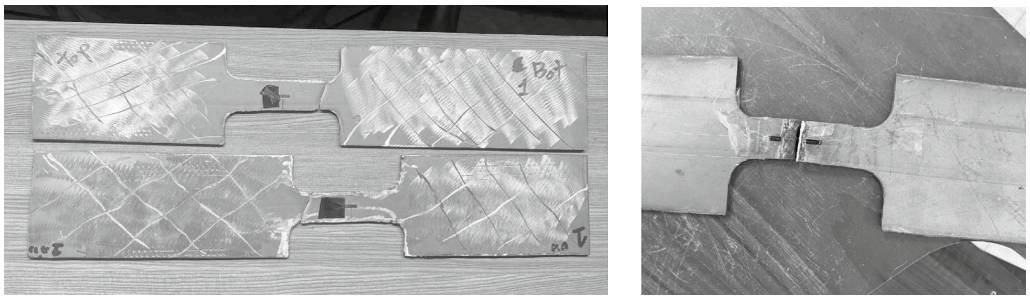

(a) The continuous sample (b) The welded sample

Fig. 5 Failure of the test samples

2.3 Preparation of the Concrete Specimens

The concrete specimens were prepared to conform with the shape of the cold-formed steel sections that are available in the market, so that no special prefabrication was needed for making the jackets. Based on the shape of the C20024 section, the test specimens were of a rectangular shape with all four round corners. The cross sections were of 130 mm × 200 mm, with the corner radius of 5 mm. The heights were 300 mm.

To prepare all test specimens, the prefabricated cold-formed steel jackets were also utilized as molds to create concrete specimens of a predefined size. The molds, which also served as the jackets, were built of two cold-formed steel lipped channel sections with the lip portions cut off (cf. Fig. 1 (right)). The two parts were then attached to the base plate to form a closed portion. All the assemblies were made by tack welding, to prevent concrete leakage during placement. The concrete was poured into these temporary molds and left to set before removing the molds. The molds, which would subsequently be used as jackets for the specimens, were labeled with symbols so that they could be fitted to their matching concrete specimens.

2.4 Preloading

Assuming a factor of safety of two, the axial load levels were selected not to exceed half of its ultimate axial capacity, in order to be within the design limit, according to ACI 318-19 (2019). In this work, three preload levels were selected for the test, including 0% (no preload), 25% and 50%. The preloads were based on the expected axial capacity of the concrete specimens, determined from $0.85f_c'A_c$, where f_c' and A_c refer to the compressive strength of the standard cylindrical concrete samples and the cross section of the concrete specimen.

To apply the required axial compressive preload, the concrete specimens were set in a specially designed steel frame system made up of two 35-mm thick plates and four high strength steel rods. A strain gauge was mounted to one side of the concrete specimen to measure the strain in the axial direction. When the loading reached the specified value, which was slightly greater than the planned preload, the steel rods were tightened up to maintain the plates in place. At this stage, when the load was removed, the concrete column tended to lose some of the axial load. The process would be started over if the retained load did not meet the desired preload.

2.5 Jacketing

The molds for concrete casting were reused as cold-formed steel jackets for the concrete specimens. This was done to ensure that the surfaces of the concrete sample and jackets fit together exactly, as no bonding agent was utilized between the two.

Before being installed on the concrete specimens, the steel jackets were cut 10 mm off the heights, so that the confined part of the specimens were left 5 mm at the top and 5 mm at the bottom ends. For jacket installation, a clamping tool was used to hold the two cold-formed steel parts as close to the surface of the concrete specimens as possible, to avoid creating space between the contact surfaces. The two cold-formed steel parts were then butt welded together. The procedure is illustrated in Fig. 6.

3 Experimental Setting

To obtain the necessary test data, each of the specimens was equipped with four strain gauges at the middle of its height. The strain gauges were aligned in axial and transverse directions, two on a narrow side and another two on a wide side of the specimens. The 70-mm strain gauges were used on the concrete surface for the unconfined specimens, whereas the 5-mm gauges were placed on the steel jackets for the confined specimens. The axial deformation of each specimen was also measured using two linear variable displacement tranducers (LVDT) with a maximum measurement size of 50 mm, along the

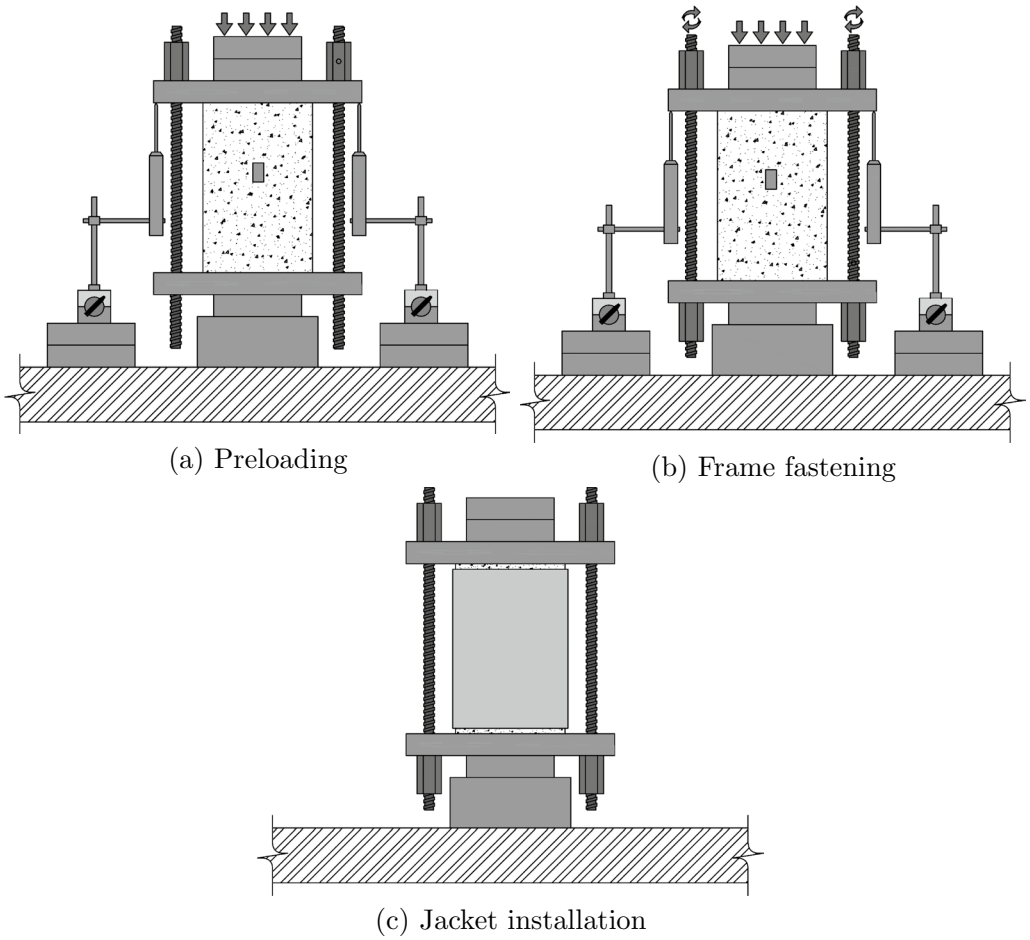

Fig. 6 Procedure for steel jacketing under preloading

loading direction. The LVDTs were used most of the time during the axial loading, and were removed when a sign of failure, either in the steel jacket or in the concrete, was noticed. The compression tests were performed on a universal testing machine. The test specimens were loaded axially through the concrete core only, not directly to the jacket. The experimental setting is shown in Fig. 7.

4 Results and Discussion

The axial compressive strengths of the test specimens are shown in Table 3. The axial compressive strengths of the unconfined specimens (Group C0) were approximately 17.9 MPa. It was shown that use of the cold-formed steel jackets could improve the axial compressive strengths of the concrete columns up around 40-65% of the original strengths.

The failure patterns observed in the unconfined specimens are shown in Fig. 8. For the confined specimens, compression failure of the concrete was observed. The crushing of concrete could also be associated with the jacket splitting after the peak load was attained, as shown for example in Fig. 9. However, if only concrete crushing failure was observed without the jacket failure, the corresponding stress–strain curve was cut off at the point to discard the rest of the curve which could end up rising again, as a result from the loading plate contacting the jacket and forming a composite section against the further loading.

4.1 Confinement Effect

The failure modes of the test specimen could imply how effective the confinement action was on the specimens. From the laboratory test, the specimens associated with jacket splitting had lower confined compressive strength than specimens that failed due to concrete compression failure. In case that the jacket could provide a very strong confinement to the concrete, the axial strength of the concrete core could go up until it reached its axial compression capacity.

Figs. 10 and 11 show the relationships between axial stress and axial/circumferential strains of all the test

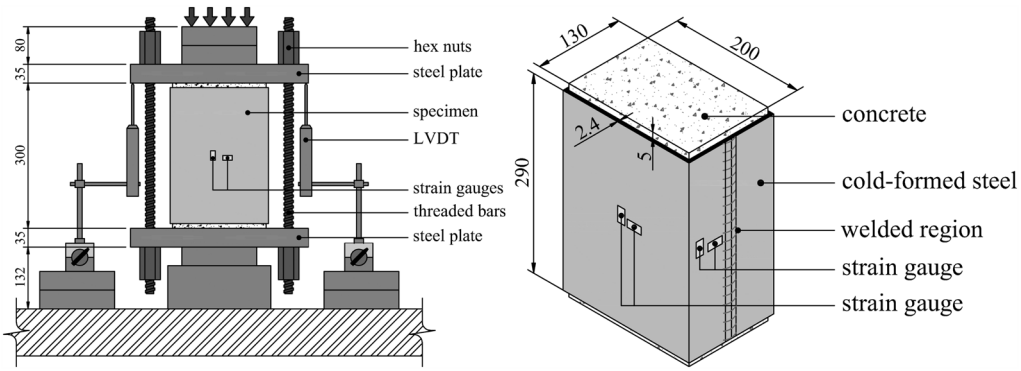

Fig. 7 Experimental setting

Table 3 The axial compressive strengths and the failure patterns of the test specimens

Group	Sample	Compressive Strength (MPa)	Average Strength (MPa)	Remarks
C0	C0-1	16.2	17.9	Reference
	C0-2	19.0		
	C0-3	18.6		
CJ0	CJ0-1	29.0	28.6	(+60.4%)
	CJ0-2	29.0		
	CJ0-3	27.8		
CJ25	CJ25-1	26.2	26.9	(+50.7%)
	CJ25-2	25.0		
	CJ25-3	29.2		
CJ50	CJ50-1	28.9	28.8	(+61.1%)
	CJ50-2	27.9		
	CJ50-3	29.5		

Fig. 8 Example of crushing failure of the unconfined concrete specimens

Fig. 9 Example of cold-formed steel splitting accompanied with crushing failure of the confined concrete specimens

specimens, measured by the axial strain gauges and the circumferential strain gauges. There, the axial compressive strains are given as positive values, while the circumferential tensile strains are denoted as negative values. The stress–strain curves on the right side of the y-axis refer to relationships between the axial stress and the axial strain, and the curves on the left side of the y-axis refer to relationships between the axial stress and the circumferential strain. It should be noted that, the strains were measured using the strain gauges attached on the concrete sides for the unconfined specimens, and using the strain gauges attached on the steel jackets for the confined specimens. The level of the ultimate axial compressive strain of unconfined core concrete was in the range of 0.0020—0.0025. The level of the ultimate axial compressive strain in the steel jacket was in the range of 0.0004 to 0.0006, regardless of the preload level equivalent to the level of axial compressive stress of 81–122 MPa in the steel jacket. The level of the ultimate circumferential tensile strain in the steel jacket was in the range of 0.002 to 0.005 equivalent to the level of axial stress of 408-610 MPa in the steel jacket.

In Fig. 12, the developed circumferential and axial strains in the cold-formed steel jacket are plotted against the axial strains in the core concrete determined from the LVDTs. The level of the ultimate axial compressive strain of confined concrete was in the range of 0.006—0.008. It

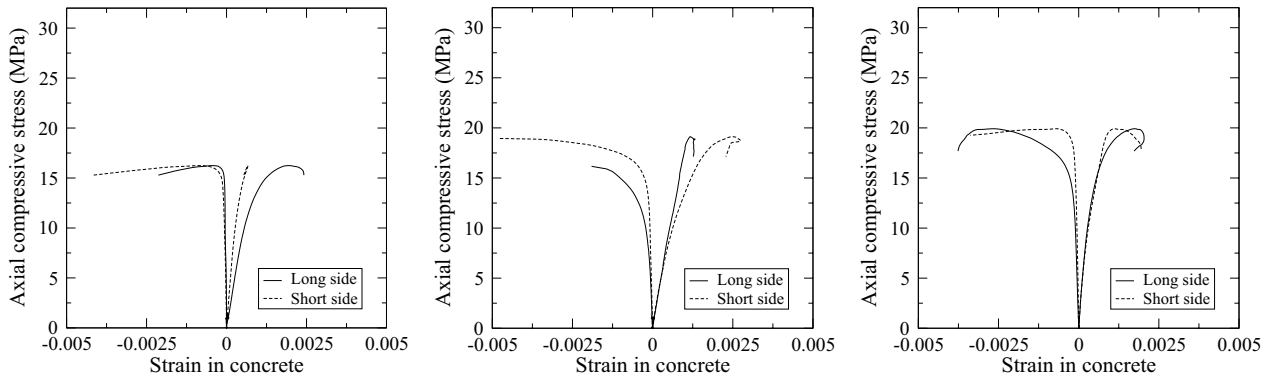

Fig. 10 Stress–strain curves for the unconfined specimens

was observed that the axial strain in the steel jacket was much less than the circumferential tensile strain in steel jacket, indicating the domination of the confinement action over the axial resistance action. The axial strains obtained from the steel jacket showed large differences in comparison of the core concrete as shown in Fig. 12. The jacket did not deform axially together with the inner concrete core. It was likely that the contact between the jacket and the core relied only on friction at the concrete–jacket interface which could be increased with the lateral expansion of the concrete core. However, the friction was likely to be very marginal, in comparison to the case where the bonding material was applied (Khamthong, 2012; Pannachet and Boonpichetvong, 2019). It was also observed that, during the compressive loading, the lateral deformation of all the specimens appeared to be very small in the beginning. The larger lateral expansions were revealed in the short sides than in the long sides of the specimens. The result was in agreement with the past observation, such as those in Saleem et al. (2018).

4.2 Preload Effect

From Table 3, the axial compressive strength of the concrete columns could be increased by cold-formed steel jacketing. However, the axial compressive strengths of the confined specimens under different preload conditions did not provide any clear correlation with the preload levels. Although the declining compressive strengths were expected as the preload level increased (Pan et al., 2017; Micelli et al., 2021; Lu et al., 2022), the strength did not show any obvious relation to the preload level, as shown in Fig. 13. To seek an explanation, one might notice in Fig. 12 (right) that the circumferential strains in the steel jackets started to increase earlier when the specimens were applied with higher preloads. The present unbonded jacketing technique might leave some very small space between the jacket and the concrete core, which could hardly be in control during the jacket installation, since no interfacial material was applied between the concrete core and the jacket. With the current technique, the imposed preload conditions did not affect the improved strength of the studied concrete specimens. The ideal confining mechanism was observed to be partially lost due to the limitation of the adopted unbonded jacketing technique. Regardless of the preload ratio level investigated, the lowest enhanced strength ratio was approximately 1.4.

5 Comparative Analysis of Existing Predictive Equations for Confined Concrete

For analysis of the laboratory test results, five sets of equations for predicting the compressive strengths of confined concrete columns are used for comparisons. The first set of equations is suggested in the ACI 440.2R-17 standard (2017) that was originally derived for predicting the compressive strength of the FRP-confined concrete, the second set is from the research by Pan et al. (2017) in which the preload effect is also included in the FRP-confined concrete model, the third set is taken from the experimental results of the concrete specimens confined with the thinner version of the cold-formed steel by Khamthong (2012), the fourth set is the proposed equation for predicting strength of concrete-filled steel tubes (Gao et al., 2022), and the final is the model from Mander et al. (1988) originally formulated for concrete confined by reinforcing steel stirrups. The models are denoted as Models (a), (b), (c), (d), and (e), respectively.

Most of the selected models are based on the relationship between the compressive strength of the confined concrete and the lateral confining pressure, in the form of

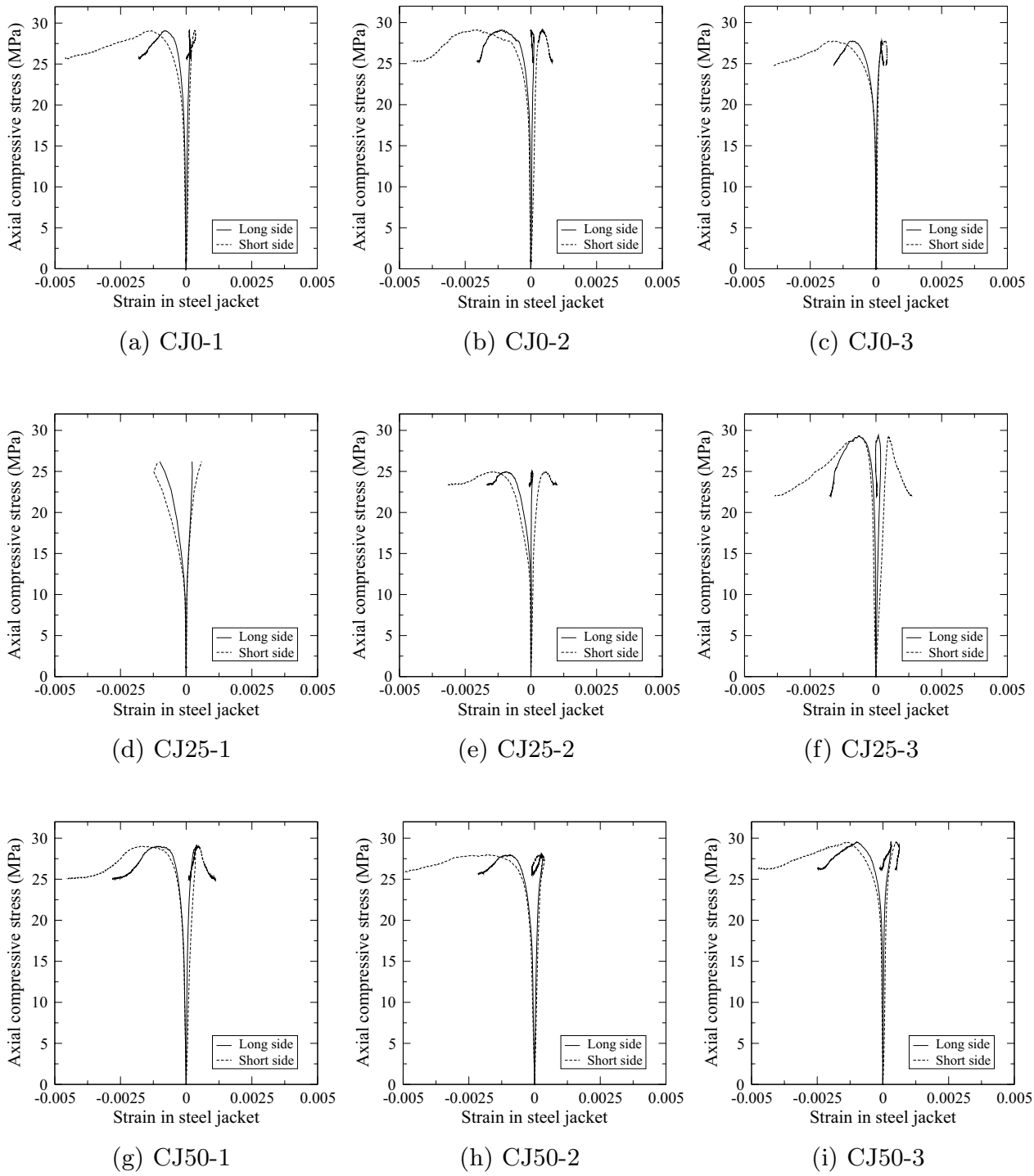

Fig. 11 Stress–strain curves for the confined specimens

$$\frac{f'_{cc}}{f'_{co}} = 1 + k\frac{f_l}{f'_{co}}, \tag{1}$$

where f'_{cc} is the axial compressive strength of the confined concrete column, f'_{co} is the axial compressive strength of the concrete column without confinement, and k the confinement coefficient. The lateral confining pressure for an equivalent circular section column f_l, with the equivalent diameter of D_e is computed from

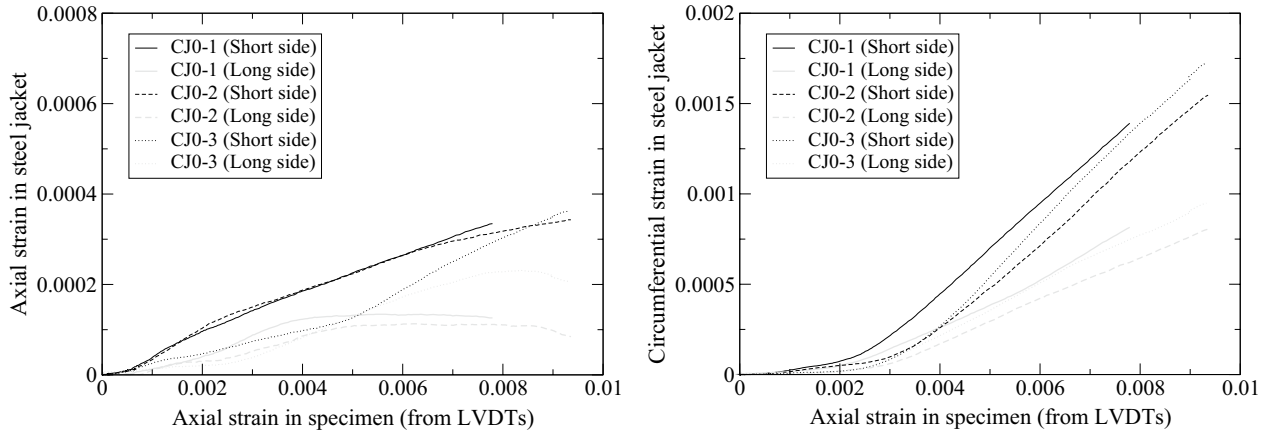

(a) Non-preloaded specimens (CJ0)

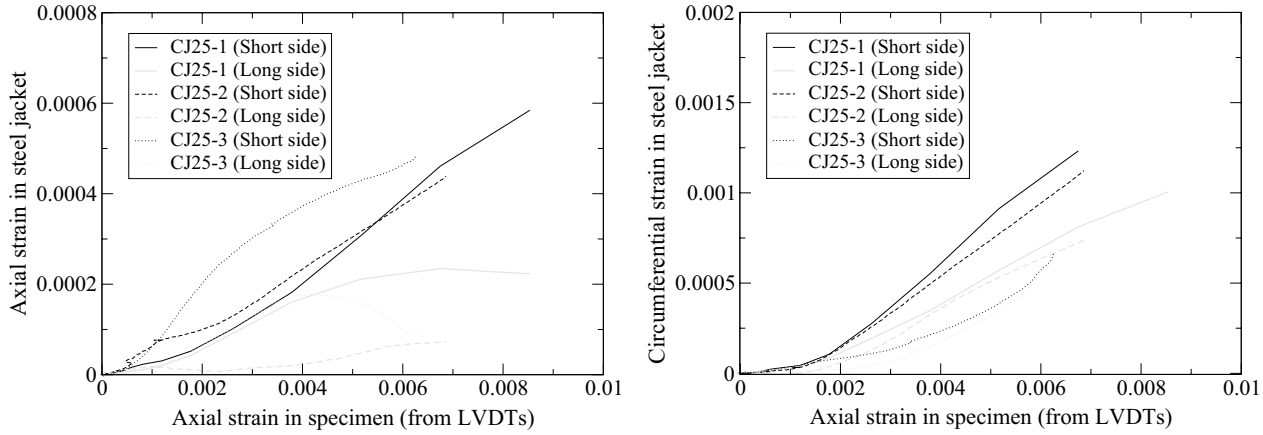

(b) 25% preloaded specimens (CJ25)

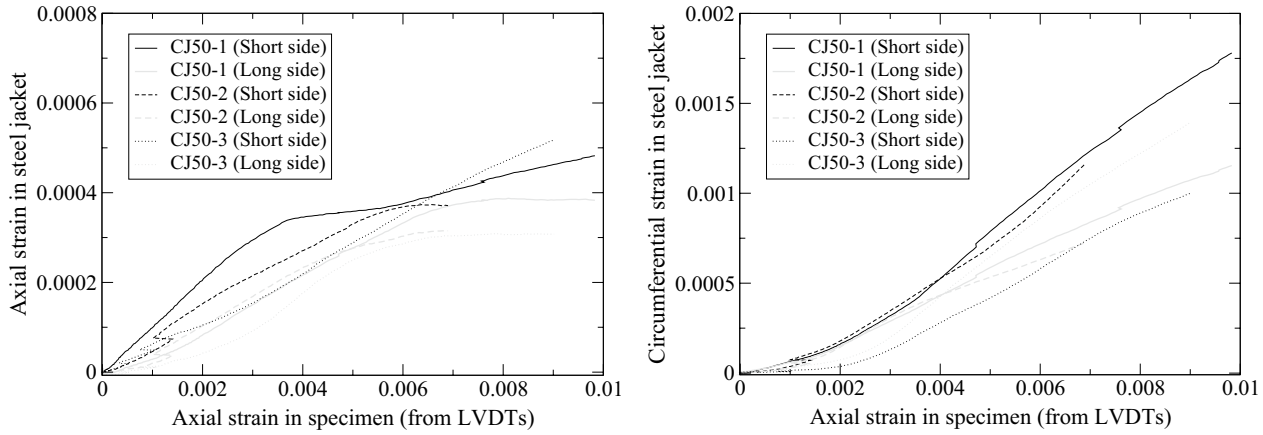

(c) 50% preloaded specimens (CJ50)

Fig. 12 Development of axial and circumferential strains in the cold-formed steel jacket

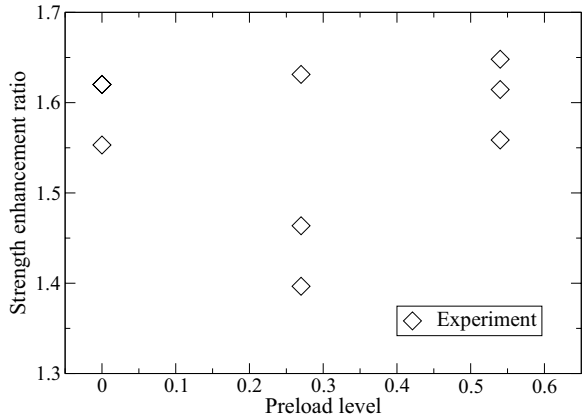

Fig. 13 Relationship between the strength enhancement ratio and the preload ratio

$$f_l = \frac{2nf_\theta t}{D_e}, \tag{2}$$

where n is the number of layers of the confining material of the thickness t and f_θ is the tensile stress in the circumferential direction. For a rectangular section of $b \times h$ with a small corner radius of r_c, the equivalent diameter may be estimated as:

$$D_e = \sqrt{b^2 + h^2}. \tag{3}$$

It is noted that f'_{cc}/f'_{co} denotes the strength enhancement ratio and f_l/f'_{co} is known as the confinement ratio.

Specific details for all the selected predictive equations are given as follows:

5.1 Predictive Equation for FRP-Confined Concrete

The standard equation given in ACI 440.2R-17 (2017) is mainly based on the research work of Lam and Teng (2003), which was derived from the carbon fiber-reinforced polymer (CFRP)-confined concrete. The normalized compressive strength of a confined concrete column can be obtained from Eq.(1) using the confinement coefficient

$$k = \psi_f 3.3\kappa_a, \tag{4}$$

where the reduction factor ψ_f is taken as 0.95 and the shape factor κ_a is computed from

$$\kappa_a = \frac{A_e}{A_c}\left(\frac{b}{h}\right)^2 \tag{5}$$

for a $b \times h$ rectangular section with the corner radius of r_c.

The ratio of effectively confined area A_e to the concrete area A_c is

$$\frac{A_e}{A_c} = 1 - \frac{\left(\left(\frac{b}{h}\right)(h-2r_c)^2 + \left(\frac{h}{b}\right)(b-2r_c)^2\right)}{3A_g} \tag{6}$$

for the concrete column with the gross sectional area A_g. Note that, if there is no longitudinal steel reinforcement in the column, A_c is equal to A_g.

5.2 Predictive Equation for FRP-Confined Concrete With Preload

Based on the research of Pan et al. (2017), the proposed confinement coefficient for a non-circular FRP-confined concrete specimens depends on the preload factor k_f, the corner (stress concentration) factor k_c and the shape (effective confinement) factor k_s, as confinement coefficient considering preload effect

$$k = 5.56k_f k_c k_s, \tag{7}$$

where

$$k_f = \left(1.0 - p^{2.12}\right)^{0.86}, \tag{8}$$

$$k_c = 0.30 + 0.35\left(\frac{2r_c}{D_e}\right)^{0.38}, \tag{9}$$

$$k_s = \frac{b}{h} \cdot \frac{bh - 0.86{r_c}^2 - \frac{1}{3}\left[(h-2r_c)^2 + (b-2r_c)^2\right]}{bh - 0.86{r_c}^2}. \tag{10}$$

The preload ratio p is defined as the ratio of the existing axial load in the column before being confined to the axial strength of the column.

5.3 Predictive Equation for Metal Sheet-Confined Concrete

From the experimental test of Khamthong (2012), the plain rectangular concrete specimens were confined with 1–3 layers of G300 metal sheet (cold-formed steel sheet) with the use of epoxy resins as the bonding material. From the experimental results, the confinement coefficients (cf. k in Eq. (1)) could be obtained by fitting each set of data points with a linear trend line. For the 22 MPa concrete specimen of 109 mm × 162 mm rectangular shape, i.e., the $b : h$ ratio is approximately 0.67, the confinement coefficient k was found to be 4.316.

This equation with the proposed coefficient was selected for comparison with the experimental result of the present study due to three reasons. Firstly, the equation was obtained from the concrete specimens confined with cold-formed steel. Although the thin sheet material might be regarded a different form of cold-formed steel and the confining system in Khamthong (2012) relied on the bonding material, it is nonetheless quite comparable

to the material used in the current investigation. Secondly, the concrete strengths of the specimens in their study and the present study were considerably closed. Thirdly, the aspect ratios of the cross sections of the specimens in their investigation and the current study were almost similar.

5.4 Predictive Equation for Concrete-Filled Steel Tube

According to the research paper by Gao et al. (2022), a confinement coefficient for the system of concrete-filled steel tube stub depending on various sectional shapes can be computed from

$$k = \frac{2(1-2\alpha)+\pi\alpha+0.5\pi t/D}{4\alpha(1-2\alpha)+(1-2\alpha)^2+\pi\alpha^2}, \tag{11}$$

where α is the corner radius (r) to steel tube width (D) ratio. It should be noted that, in this paper, the original equation was modified by replacing the steel tube width by the equivalent diameter of the column D_e (cf. Equation(3)).

5.5 Predictive Equation for Concrete Confined by Reinforcing Steel

Based on many test results on circular, square and rectangular reinforced concrete columns, Mander et al. (1988) proposed a prediction equation in a nonlinear form

$$\frac{f'_{cc}}{f'_{co}} = 2.254\sqrt{1+7.94\frac{f_l}{f'_{co}}} - 2\frac{f_l}{f'_{co}} - 1.254. \tag{12}$$

To understand the components in the given confinement equations, the confinement coefficients for the aforementioned predictive equations are collected in Table 4. The original coefficients from these equations are originally based on axial compression experiments of cylindrical concrete specimens, the shape of which the most effective confinement effects are expected. As the confinement effect depends on many factors including shapes of concrete specimens and level of sustained axial loads, the coefficients may be modified by using some multiplying factors that give reduction in strength enhancement.

From the selected models, the predictive equations can be categorized into two groups depending on types of the confining materials. While Models (a) and (b) are formulated from the FRP-confined concrete, Models (c), (d), and (e) are based on steel, either in the form of thin sheet, tube, or rebars. From Table 4, the factor that exhibited the most impact on strength reduction was the shape factor. For the test specimens in the current study, contribution of the shape factors (cf. Model (a) and (b)) reduced the improved strengths greatly; the resulting confinement coefficients were down to only approximately 20% for the FRP-confined concrete. On the other hand, according to Model (b), existence of preload might decrease the axial strength of the specimens not as much; the retained strengths are around 94% and 76% for the sustained axial load of 25% and 50%, respectively. These effects, however, may not be the same for the steel confinement. Unfortunately, the relevant variables were not clearly separated in Model (c), (d) and (e).

In order to compare the experimental results to the predictive models, the strength enhancement ratios (f'_{cc}/f'_{co}) should be plotted against the confinement ratios (f_l/f'_{co}). From the experimental results, the lateral confining pressure for each specimen was computed by inserting f_θ in Eq.(2). To determine the value of f_θ, the circumferential strain at the peak load was obtained from the strain gauge that was aligned in the horizontal direction. Correspondingly, the circumferential stress emerging in the cold-formed steel jacket could be determined from the stress–strain relationship of the coupon specimen from the tensile testing (cf. Section 2.2). For these non-circular shaped specimens, the circumferential

Table 4 Summary of confinement coefficients for the test specimens

Model	Original confinement coefficient	Multiplying factors		Final confinement coefficient	Remarks
(a)	$k_0 = 3.30$	$\psi_f = 0.95$	(reduction factor)	$k = 0.5492$	
		$\kappa_a = 0.1752$	(shape factor)		
(b)	$k_0 = 5.56$	$k_f = 1$	(preload factor)	$k = 0.5151$	for $p = 0.00$
		$k_f = 0.9462$	(preload factor)	$k = 0.4874$	for $p = 0.25$
		$k_f = 0.7621$	(preload factor)	$k = 0.3926$	for $p = 0.50$
		$k_c = 0.4049$	(corner factor)		
		$k_s = 0.2288$	(shape factor)		
(c)	-	-	-	$k = 4.316$	
(d)	-	-	-	$k = 1.999$	

strain could vary depending on location on the jacket. In the experiment, the strain gauges were placed in the circumferential direction; a gauge was located next to the weld line on the short side and at around one-third of the width measured from the corner on the long side of the jacket. Since the strain appeared larger on the short side and therefore controlled the failure mechanism, it was used for determination of the stress in the jacket. The lateral confining pressures for all the test specimens are collected in Table 5.

From the experimental results, the axial strength enhancement ratios of the test stub columns were plotted against the corresponding confinement ratios, as well as the predicted values obtained from the various models (a) to (e), as shown in Fig. 14. The predicted to experimentally obtained strength ratios were also computed and compared using the predictive models (a) to (e), as shown in Table 6. The results indicated that the strength improvement obtained using the unbonded cold-formed steel jacketing technique conformed very much to the predictive model (d) originally proposed for the concrete-filled tubes.

It can be seen that Model (a) and (b) gave predicted strengths that were much lower than the strengths that were obtained from the experiment. The equations provided too conservative values for predicting the strength of the jacketed concrete specimens, implying that the predictive equations based on the FRP confinement might not be applicable for the cold-formed steel-confined concrete. On the other hand, the strength predictions from Model (c) and Model (e), which are based on confinement using metal sheet confinement and steel stirrups, gave overestimated strength prediction. An explanation for the overestimation in the metal sheet model (Model (c)) may be due to the use of bonding material which helps increase the axial strengths in two ways. The bonding material acted as the interfacial material that filled up the space between the core and the confining material so

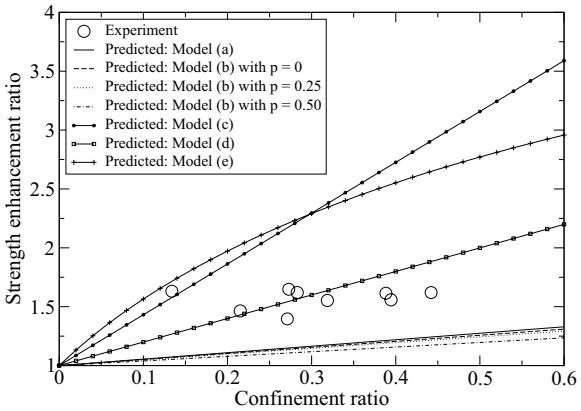

Fig. 14 Comparison of the strength enhancement ratio–confinement ratio relationships obtained from the experiment and the predictive equations

that resistance to the lateral expansion could be initiated fully from the beginning. The bonding material could also bring about the resistance in the metal sheet jacket in the axial direction along with the core concrete, as also observed in Pannachet and Boonpichetvong (2019). Without the bonding material, the predicted strength could be lowered. However, the predictive equations of Model (c) and Model (e) might still be used, with introduction of a reduction factor to account for the lack of bonding substance. Among all the models, the model based on the concrete-filled tube (Model (d)) seems to be the best at predicting the experimental data. Despite the fact that the axial load resistance of the filled tube relies on the composite action of the tube as well as the core, there was no bonding substance between the concrete and the steel tube.

The present study is limited to the confinement behavior of the low-strength concrete specimens of a certain size, using the cold-formed steel jacket of a certain thickness. The assembly of the jacket has also been based on

Table 5 The lateral confining pressure at the maximum load in the test specimens

Specimen	Axial compressive strength (MPa)	Circumferential strain in jacket	Circumferential stress in jacket (MPa)	Lateral confining pressure (MPa)
CJ0-1	29.0	0.0014	250.92	5.05
CJ0-2	29.0	0.0022	392.28	7.89
CJ0-3	27.8	0.0016	282.72	5.69
CJ25-1	26.2	0.0011	190.84	3.84
CJ25-2	25.0	0.0014	240.31	4.84
CJ25-3	29.2	0.0007	118.74	2.39
CJ50-1	28.9	0.0020	344.57	6.93
CJ50-2	27.9	0.0020	349.87	7.04
CJ50-3	29.5	0.0014	242.08	4.87

Table 6 Ratio of predicted to obtained axial strengths ($f'_{cc,predict}/f'_{cc,exper}$)

Model	(a)	(b)	(c)	(d)	(e)
Source	ACI 440.2R (2017)	Pan et al. (2017)	Khamthong (2012)	Gao et al. (2022)	Mander et al. (1988)
Confining material	FRP sheet	FRP sheet with preload	Metal sheet	Concrete filled steel tube	Steel stirrups
Interface bond	Epoxy resins	Epoxy resins	Epoxy resins	None	Cast in concrete
Sample	Ratio of predicted to obtained axial strengths ($f'_{cc,predict}/f'_{cc,exper}$)				
CJ0-1	0.71	0.71	1.37	0.97	1.38
CJ0-2	0.77	0.76	1.79	1.16	1.63
CJ0-3	0.76	0.75	1.53	1.05	1.51
CJ25-1	0.76	0.75	1.32	0.98	1.38
CJ25-2	0.82	0.81	1.55	1.10	1.58
CJ25-3	0.66	0.65	0.97	0.78	1.05
CJ50-1	0.75	0.71	1.66	1.10	1.56
CJ50-2	0.78	0.74	1.73	1.15	1.63
CJ50-3	0.70	0.67	1.32	0.94	1.34

technique of welding, without any bonding material to join jackets to the concrete core. The study can be considered as the first start on development of the practical cold-formed steel jacketing system. After a more detailed investigation of the necessary model parameters is available, the experimental results can be enriched with some numerical analyses. There are also some other interesting issues to be investigated further. Finding efficient techniques of jacket assemblies to facilitate quick installation of the jacketing system can bring innovations in renovation practice. Based on the results from the present study, the cold-formed steel jackets were used as casting molds to facilitate fitting of the concrete core to the post-installed jacket, an efficient technique to get a perfect jacket fit is still needed for practical cases. Further investigation into the preload and size effects on the strengthening mechanism is also necessary. It has been reported in the area of seismic retrofitting of structures that the initial preloads can deteriorate the seismic performance of the jacketed columns (Vandoros and Dritsos, 2006; Shi et al., 2022). The level of axial compression also limits the amount of confining reinforcement to be provided in order to enhance member ductility effectively (Yuen et al., 2016). There is also a size effect issue involving slenderness and cross section of the columns that can affect the seismic safety of structures (Hung et al., 2024).

6 Conclusions

Cold-formed steel (CFS) is an appealing confining material for concrete members due to its high strength and lightweight design, which allows for simple installation. The test results of CFS-confined concrete columns under axial compression can be summarized as follows:

1. The compressive strength of the cold-formed steel jacketed concrete columns ranges between 25–29.5 MPa, representing the increases in strength of approximately 40-65%, when compared to the reference concrete column with an average compressive strength of approximately 17.85 MPa.
2. During the axial loading, the circumferential strain measurement on the cold-formed steel jacket confirms the main role of the jacket in laterally confining the concrete core. Without any bonding material, the jacket does not exhibit axial deformation along with the core. The increased axial strength of the concrete specimen is mainly due to confinement action.
3. From the test results, the variation of 0-50% sustained axial load in the concrete column before being jacketed with cold-formed steel does not seem to affect the axial compression capacity of the concrete specimens.
4. Using five currently available strength predictive equations, the measured strength enhancement ratio and the confinement ratio of the tested specimens are compared. The performance of the unbonded cold-formed steel jacketing technique is found to

closely match the predictive confinement model of the concrete-filled tubes.

Acknowledgements
The authors would like to thank the team members at KKU Structural Engineering Laboratory for providing their assistantships in setting and conducting the laboratory experiment.

Author contributions
AW conducted the experimental test, analyzed the test results and prepared the manuscript draft. TP conceptualized and designed the work, supervised the experimental test and edited the manuscript. MB validated the data and revised the manuscript. All authors have read and agreed to the published version of the manuscript.

Funding
The research is financed by KKU Civil engineering research fund Grant No. 5/2562, Khon Kaen University, Thailand.

Availability of data and materials
All data generated or analyzed during this study are included in this published article.

Declarations

Competing interests
The authors declare no conflict of interest.

Received: 22 March 2024 Accepted: 23 June 2024
Published online: 16 September 2024

References

Abo-Zaid, L., Hassan, A., & Abdel-Hafez, L. M. (2019). Repairing post-heated L-shaped RC columns with advanced thin concrete jacketing. *Construction and Building Materials, 221*, 573–585. https://doi.org/10.1016/j.conbuildmat.2019.06.101

ACI 318-19: (2019). Building Code Requirements for Structural Concrete and Commentary. ACI Committee 318, American Concrete Institute

ACI 440.2R-17: (2017). Guide for the Design and Construction of Externally Bonded FRP Systems for Strengthening Concrete Structures. ACI Committee 440, American Concrete Institute

Almusallam, T. H. (2007). Behavior of normal and high-strength concrete cylinders confined with E-glass/epoxy composite laminates composite laminates. *Composites: Part B, 38*(5), 629–639. https://doi.org/10.1016/j.compositesb.2006.06.021

AS 1397:2021: (2021). Continuous Hot-dip Metallic Coated Steel Sheet and Strip - Coatings of Zinc and Zinc Alloyed with Aluminium and Magnesium. Standards Australia, SAI Global

AS/NZS 1365:1996 (R2016): (2016). Tolerances for Flat-rolled Steel Products. Standards Australia & Standards New Zealand, SAI Global, Australia & New Zealand

ASTM C39/C39M-21: (2021). Standard Test Method for Compressive Strength of Cylindrical Concrete Specimens. ASTM International, West Conshohocken, PA, USA

ASTM C469/C469M-22: (2022). Standard Test Method for Static Modulus of Elasticity and Poisson's Ratio of Concrete in Compression. ASTM International, West Conshohocken, PA, USA

ASTM E8/E8M-22: (2022). Standard Test Methods for Tension Testing of Metallic Materials. ASTM International

Belal, M. F., Mohamed, H. M., & Morad, S. A. (2015). Behavior of reinforced concrete columns strengthened by steel jacket. *HBRC Journal, 11*(2), 201–212. https://doi.org/10.1016/j.hbrcj.2014.05.002

Boonpichetvong, M., Pannachet, T., & Pinitkarnwatkul, S. (2016). Finite element modeling of concrete specimens confined with metal sheet strips. *International Journal of Technology, 7*, 1132–1140. https://doi.org/10.14716/ijtech.v7i7.4875

Boonpichetvong, M., Pannachet, T., Pinitkarnwatkul, S., & Askes, H. (2018). Concrete columns with discrete confinement by metal sheets subjected to uniaxial compression: derivation toward design rule. *Engineering and Applied Science Research, 45*(1), 56–64. https://doi.org/10.14456/easr.2018.2

Chen, M. T., Zhang, T., & Young, B. (2023). Behavior of concrete-filled cold-formed steel built-up section stub columns. *Thin-Walled Structures, 187*, 110692. https://doi.org/10.1016/j.tws.2023.110692

Chin, C. L., Ma, C. K., Tan, J. Y., Ong, C. B., Awang, A. Z., & Omar, W. (2019). Review on development of external steel-confined concrete. *Construction and Building Materials, 211*, 919–931. https://doi.org/10.1016/j.conbuildmat.2019.03.295

Choi, E. (2009). A new steel jacketing method for RC columns. *Magazine of Concrete Research, 61*(10), 787–796. https://doi.org/10.1680/macr.2008.61.10.787

Elsayed, M., Abou Elmaaty, M., & Mohamed, R. (2023). Retrofitting of post-heated RC columns using steel fiber reinforced self-compacting concrete jackets. *Construction and Building Materials, 400*, 132637. https://doi.org/10.1016/j.conbuildmat.2023.132637

Ersoy, U., Tankut, A. T., & Suleiman, R. (1993). Behavior of jacketed columns. *ACI Structural Journal, 90*(3), 288–293. https://doi.org/10.14359/4236

Ferrotto, M. F., Cavaleri, L., & Papia, M. (2018). Compressive response of substandard steel-jacketed RC columns strengthened under sustained service loads: from the local to the global behavior. *Construction and Building Materials, 179*, 500–511. https://doi.org/10.1016/j.conbuildmat.2018.05.247

Ferrotto, M. F., Fischer, O., & Cavaleri, L. (2018). A strategy for the finite element modeling of FRP-confined concrete columns subjected to preload. *Engineering Structures, 173*, 1054–1067. https://doi.org/10.1016/j.engstruct.2018.07.047

Ferrotto, M. F., Fischer, O., & Niedermeier, R. (2018). Experimental investigation on the compressive behavior of short-term preloaded carbon fiber reinforced polymer-confined concrete columns. *Structural Concrete, 19*(4), 988–1001. https://doi.org/10.1002/suco.201700072

Ferrotto M.F., Pradhan, B., & Cavaleri L. (2021). The role of the sustained loads on the bearing capacity of reinforced concrete columns retrofitted by steel jackets. In: Papadrakakis, M., Fragiadakis, M. (eds.) Proceedings of the 8th International Conference on Computational Methods in Structural Dynamics and Earthquake Engineering Methods in Structural Dynamics and Earthquake Engineering (COMPDYN 2015), Athens, Greece. https://doi.org/10.7712/120121.8568.19548

Gao, Q., Li, J., Zhou, J., Lai, X., & Hwang, H. (2022). A unified model for compressive strength of concrete-filled steel tube short columns with various symmetric sections. *Journal of Building Engineering, 61*, 105227. https://doi.org/10.1016/j.jobe.2022.105227

Harrat, O., Hadidane, Y., Anas, S. M., Sor, N. H., Deifalla, A. F., Awoyera, P. O., & Gouider, N. (2024). Nonlinear study on the mechanical performance of built-up cold-formed steel concrete-filled columns under compression. *CMES-Computer Modeling in Engineering & Sciences, 139*(3), 3435–3465. https://doi.org/10.32604/cmes.2023.044950

Huang, W. F., Shao, Y. B., & Hassanein, M. F. (2023). Behaviour and confinement-based direct design of concrete-filled cold-formed stiffened steel tubular short columns. *Journal of Constructional Steel Research, 202*, 107773. https://doi.org/10.1016/j.jcsr.2022.107773

Hung, C. C., Yuen, T. Y., & Mosalam, K. M. (2024). Full-scale cyclic testing of slender RC columns bent in double curvature under high axial load. *Journal of Building Engineering, 82*, 108186. https://doi.org/10.1016/j.jobe.2023.108186

JIS G 3323:2022: (2022). Hot-Dip Zinc-Aluminium-Magnesium Alloy-Coated Steel Sheet And Strip. Japanese Industrial Standards, Japanese Standards Association

Khamthong, M. (2012). Axial compression strengthening of concrete columns confined by metal sheet. Master's Thesis, Khon Kaen University, Thailand.

Kumar, J., & Ramasamy, V. (2017). Confinement effect on strength of concrete columns by using cold-formed steel tubes. *Journal of Structural Engineering (India), 44*(5), 475–485.

Lai, B. L., Zhang, M. Y., Chen, Z. P., Liew, J. R., & Zheng, Y. Y. (2023). Axial compressive behavior and design of semi-precast steel reinforced concrete

composite columns with permanent ecc formwork. *Structures, 33*, 105130. https://doi.org/10.1016/j.istruc.2023.105130
Lai, B. L., Zhang, M. Y., Zheng, X. F., Chen, Z. P., & Zheng, Y. Y. (2023). Experimental study on the axial compressive behaviour of steel reinforced concrete composite columns with stay-in-place ecc jacket. *Journal of Building Engineering, 68*, 106174. https://doi.org/10.1016/j.jobe.2023.106174
Lai, B. L., Zheng, X. F., Fan, S. G., & Chang, Z. Q. (2024). Behavior and design of concrete filled stainless steel tubular columns under concentric and eccentric compressive loading. *Journal of Constructional Steel Research, 213*, 108319. https://doi.org/10.1016/j.jcsr.2023.108319
Lam, L., & Teng, J. G. (2003). Design-oriented stress-strain models for FRP-confined concrete. *Construction and Building Materials, 17*(6–7), 471–89. https://doi.org/10.1016/S0950-0618(03)00045-X
Lin C.Y. (1988). Axial capacity of concrete infilled cold-formed steel columns. In: Proceeding of the International Specialty Conference on Cold-Formed Steel Structures, vol. 2, pp. 593–660
Lu, S., Wang, J., Yang, J., & Wang, L. (2022). Numerical analysis of preloaded FRP-strengthened concrete columns under axial compression. *Construction and Building Materials, 357*, 129297. https://doi.org/10.1016/j.conbuildmat.2022.129297
Mander, J. B., Priestley, M. J. N., & Park, R. (1988). Theoretical stress-strain model for confined concrete. *Journal of structural engineering, 114*(8), 1804–1826.
Men, P., Di, J., Qin, F., Lin, E., Wang, J., & Peng, X. (2024). Experimental investigation on axial compression behaviour of cold-formed thick-walled steel tubes. *Journal of Constructional Steel Research, 214*, 108431. https://doi.org/10.1016/j.jcsr.2023.108431
Micelli, F., Cascardi, A., & Aiello, M. A. (2021). Pre-load effect on CFRP-confinement of concrete columns: Experimental and theoretical study. *Crystals, 11*(2), 177. https://doi.org/10.3390/cryst11020177
Minafó, G. (2015). A practical approach for the strength evaluation of RC columns reinforced with RC jackets. *Engineering Structures, 85*, 162–169. https://doi.org/10.1016/j.engstruct.2014.12.025
Mirmiran, A., Shahawy, M., Samaan, M., & El Echary, H. (1998). Effect of column parameters on FRP confined concrete. *Journal of Composites for Construction, 2*(4), 175–185. https://doi.org/10.1061/(ASCE)1090-0268(1998)2:4(175)
Pan, Y., Guo, R., Li, H., Tang, H., & Huang, J. (2017). Analysis-oriented stress-strain model for FRP-confined concrete with preload. *Composite Structures, 166*, 57–67. https://doi.org/10.1016/j.compstruct.2017.01.007
Pannachet, T., & Boonpichetvong, M. (2018). Axial compressive strength of metal sheet confined concrete cylinders based on various concrete strengths. *Civil Engineering Journal, 4*(11), 2529–2538. https://doi.org/10.28991/cej-03091178
Pannachet, T., & Boonpichetvong, M. (2019). Numerical investigation of axial strength development in metal sheet confined concrete. *Engineering Journal of Research and Development, 30*(2), 33–46.
Papanikolaou, V. K., Stefanidou, S. P., & Kappos, A. J. (2013). The effect of preloading on the strength of jacketed R/C columns. *Construction and Building Materials, 38*, 54–63. https://doi.org/10.1016/j.conbuildmat.2012.07.100
Positong, A., Pannachet, T., & Boonpichetvong, M. (2018). Discrete confinement by metal sheet strips on concrete columns under axial compression. *International Journal of GEOMATE, 15*(52), 184–191. https://doi.org/10.21660/2018.52.27093
Saleem, S., Pimanmas, A., & Rattanapitikon, W. (2018). Lateral response of PET FRP-confined concrete. *Construction and Building Materials, 159*, 390–407. https://doi.org/10.1016/j.conbuildmat.2017.10.116
Shahawy, M., Mirmiran, A., & Beitelman, T. (2000). Tests and modeling of carbon-wrapped concrete columns. *Composites: Part B, 31*(6–7), 471–80. https://doi.org/10.1016/S1359-8368(00)00021-4
Shehata, L. A. E. M., Carneiro, L. A. V., & Shehata, L. C. D. (2002). Strength of short concrete columns confined with CFRP sheets. *Material and Structures, 35*(245), 50–58.
Shi, D., & He, Z. (2009). Short-term axial behavior of preloaded concrete columns strengthened with fiber reinforced polymer laminate. In Y. Yuan, J. Cui, & H. A. Mang (Eds.), *Computational Structural Engineering* (pp. 1089–1098). Dordrecht: Springer.
Shi, Y., Yuan, G., & Zhu, H. (2022). Effect of axial compression ratio on seismic and self-centering performance of unbonded prestressed concrete columns. *Advances in Civil Engineering, 2022*, 1–13. https://doi.org/10.1155/2022/7346620
Takeuti, A. R., Hanai, J. B., & Mirmiran, A. (2008). Preloaded RC columns strengthened with high-strength concrete jackets under uniaxial compression. *Materials and Structures, 41*, 1251–1262. https://doi.org/10.1617/s11527-007-9323-0
Taufiq, H., & Lawson, R. M. (2020). Composite columns using perforated cold formed steel sections. *Journal of Constructional Steel Research, 167*, 105935. https://doi.org/10.1016/j.jcsr.2020.105935
Thermou, G. E., Pantazopoulou, S. J., & Elnashai, A. S. (2012). Global interventions for seismic upgrading of substandard RC buildings. *Journal of Structural Engineering, 138*(3), 387–401. https://doi.org/10.1061/(ASCE)ST.1943-541X.0000474
Vandoros, K. G., & Dritsos, S. E. (2006). Axial preloading effects when reinforced concrete columns are strengthened by concrete jackets. *Progress in Structural Engineering and Materials, 8*(3), 79–92. https://doi.org/10.1002/pse.215
Vijayan, D. S., Sivasuriyan, A., Devarajan, P., Stefańska, A., Wodzyński, L., & Koda, E. (2023). Carbon Fibre-Reinforced Polymer (CFRP) composites in civil engineering application–a comprehensive review. *Buildings, 13*(6), 1509. https://doi.org/10.3390/buildings13061509
Villar-Salinas, S., Guzmán, A., & Carrillo, J. (2021). Performance evaluation of structures with reinforced concrete columns retrofitted with steel jacketing. *Journal of Building Engineering, 33*, 101510. https://doi.org/10.1016/j.jobe.2020.101510
Wang, L., An, Y., Ding, F., Kuang, Y., Ma, Q., Tan, S., Zhang, W., Zhao, P., & Ren, E. (2021). Numerical investigation of composite behavior and strength of rectangular concrete-filled cold-formed steel tubular stub columns. *Materials, 14*(20), 6221. https://doi.org/10.3390/ma14206221
Yuen, T. Y., Kuang, J. S., & Ho, D. Y. (2016). Ductility design of RC columns. part 1: consideration of axial compression ratio. *HKIE Transactions, 23*(4), 230–244. https://doi.org/10.1080/1023697X.2016.1232179
Yu, Y., Gan, M., Zhang, Y., & Luo, L. (2024). Experimental study on horizontal low-cycle loading of high-strength concrete medium high shear wall with cold-formed steel braces. *Journal of Building Engineering, 84*, 108472. https://doi.org/10.1016/j.jobe.2024.108472
Zhang, J. H., Hassanein, M. F., Cashell, K. A., Hadzima-Nyarko, M., Xu, Y., & Shao, Y. B. (2024). Experimental and numerical investigation on the behaviour of square concrete-filled cold-formed double-skin steel stiffened tubular short columns. *Engineering Structures, 303*, 117560. https://doi.org/10.1016/j.engstruct.2024.117560

Publisher's Note

Apisith Waenpracha is a graduate student at Department of Civil Engineering, Khon Kaen University, Khon Kaen 40002, Thailand.

Tanyada Pannachet is an associate professor at Department of Civil Engineering and also a researcher at Sustainable Infrastructure Research and Development Center, Faculty of Engineering, Khon Kaen University, Khon Kaen 40002, Thailand.

Maetee Boonpichetvong is an associate professor at Department of Civil Engineering and also a researcher at Sustainable Infrastructure Research and Development Center, Faculty of Engineering, Khon Kaen University, Khon Kaen 40002, Thailand.